Available online at www.sciencedirect.com
SCIENCE DIRECT®
Chemical Engineering and Processing 43 (2004) 1449–1458
Chemical Engineering and Processing
www.elsevier.com/locate/cep

Real-time inferencing of solid–liquid phase equilibria in solution polymerization of polyethylene

Sayeed Abbas [a], Rabibrata Mukherjee [b], Sirshendu De [c], Saibal Ganguly [c,*]

[a] *Department of Chemical Engineering and Materials Science, University of Minnesota, Minneapolis, USA*
[b] *Composite Division, Central Glass and Ceramics Research Institute, Kolkata 700032, India*
[c] *Department of Chemical Engineering, Indian Institute of Technology, Kharagpur 721302, India*

Received 13 August 2003; received in revised form 26 January 2004; accepted 26 January 2004
Available online 25 March 2004

Abstract

An algorithm for the real-time prediction of multi-component solid–liquid equilibrium (SLE) in a polyethylene (PE) process flowsheet has been attempted. While most of the available literature assumes the polymer to possess a single average molecular weight and lump the entire polymer as a single component, the present work proposes to consider a polydispersed multi-component fraction, characterized by the pseudo-component approach. The SLE model has been used to study the effects of monomer and polymer polydispersity in solution polymerization process. At first, it has been validated on the solubility data of *n*-alkanes in *n*-hexane, polyethylene in M-xylene and on wax precipitation from a mixture of *n*-paraffins. The SLE model is based on perturbed chain SAFT (PC–SAFT) equation of state (EOS). An algorithm for the real-time prediction of SLE phase boundaries in solution polymerization has been subsequently presented. A simulation experiment on the polyethylene flowsheet highlighted the potential of real-time inferencing for industrial applications.

Keywords: Solid–liquid equilibria; Real-time modeling; Polyethylene

1. Introduction

In modern polymerization plants, real-time prediction of the polymerization process parameters and polymer properties has become important for stringent product quality control. Real-time inferencing also acts as a valuable early warning and decision-making tool for automated plant operation. There are four different technological routes by which polyethylene (PE) is manufactured, namely, slurry polymerization, gas phase polymerization, high pressure bulk polymerization and solution polymerization. Among these processes, slurry and gas phase polymerizations are the most widely studied processes but solution polymerization offers wider flexibilities on the product properties of the different grades of polymer. Solid–liquid equilibria (SLE) plays a pivotal role in slurry and solution polymerization. In slurry polymerization, plant operating conditions are maintained such that the polymer produced does not dissolve in the solvent used. On the other hand, in solution polymerization, the polymer produced in the reactors remains in solution and precipitation of polymer from the solution is undesirable. Polymer precipitation from the solution may lead to clogging of heat exchangers and choking of reactor pipes and connections which may lead to shutdown of the plant. Real-time monitoring of solid–liquid phase equilibria boundaries may help in prevention of plant shutdowns and costly overhauling operations. Hence for the smooth operation of a plant, real-time prediction and monitoring of SLE in the plant is important.

Two different approaches have been used by various workers over the years to model solid–liquid phase equilibria. One approach is to use excess gibbs energy models based on the local composition concept. Coutinho [4] has used this concept and correlated *n*-alkane solubility by using the NRTL and UNIQUAC models. The other approach is to use equation of states (EOS) to represent the liquid phase non-ideality. Pan and Radosz [1] have used copolymer SAFT, whereas, Coutinho et al. [7] have found the Flory free volume theory to be a good model for prediction of hydrocarbon SLE and have used the chain delta lattice

* Corresponding author. Tel.: +91-3222-283928; fax: +91-3222-282250.
E-mail address: sganguly@che.iitkgp.ernet.in (S. Ganguly).

0255-2701/$ – see front matter © 2004 Elsevier B.V. All rights reserved.
doi:10.1016/j.cep.2004.01.003

parameter model for correlating higher n-alkane solubility. Peng et al. [2] have used an equation of state previously developed for fluids containing chain like molecules, for the prediction of solid–liquid equilibria of hydrocarbons.

The general thermodynamic framework for the prediction of SLE phase boundaries has been proposed by Prausnitz et al. [3]. In this work the equation of state approach was used to capture the liquid phase non-ideality. The PC–SAFT equation of state, which is a modification of the SAFT equation of state and has proven predictive capabilities [5,6], was chosen as the EOS.

Till date, all the SLE models for polymer systems consider the polymer as a single component of unique molecular weight (equivalent to the number average or weight average molecular weight). The polydispersity of polymers has never been considered in SLE calculations in a proper perspective. Presence of other components also alters the SLE of the polymer systems significantly. Flash algorithms including equilibria of polydisperse polymers are available in literature [20,21]. Quite often the algorithms are independent of the number of pseudo-components or monomer effects. For polymerization process, the presence of monomer in the solution is inevitable which alters the SLE characteristics. In the present work, both the above aspects have been studied and the general model of SLE was applied to multi-component systems.

A real-time simulation experiment was subsequently carried out where a disturbance in the plant operation was simulated and the SLE behavior of the reaction media was mapped. The experiment demonstrated the significance of such real-time model based inferencing for an operating industrial chemical process.

2. Simulation experiment

A typical simplified flowsheet of the reaction area of a solution polymerization plant is shown in Fig. 1. The reactor series consists of a continuous stirred tank reactor (CSTR), followed by a plug flow reactor (PFR), where most of the chain termination reactions take place. Hence it is sometimes known as the trimmer reactor. It is then followed by a solution preheater which heats up the solution further before catalyst removal and the flash columns. The pressure is gradually reduced in stages in the flash columns. The overhead gas is treated and the unreacted ethylene and solvent are recycled. Three temperature indicators, shown in Fig. 1, has been used by the simulation experiment for real-time SLE predictions. The first indicator T1 is shown at the outlet of the PFR. This is the highest temperature to which the solution is exposed in the reactors. The other two indicators, T2 and T3, are at the liquid downflow streams of the two flash columns. These two indicators indicate the temperatures at which flash is occurring in the two respective flash columns. It is assumed that the temperatures of the overhead gas stream and the liquid downflow are same. The approximation is reasonable since the temperatures of the two streams in actual plant operations hardly differ by 2 °C. The system pressure before the flash columns is indicated by the pressure tag P1. P2 and P3 represents the letdown pressure after the first and second flash columns. The composition of the inlet stream to the first column can be obtained from the composition analyzer transmitter (AT) or it can be obtained from a real-time simulator hooked online to the plant distributed control system (DCS).

3. Multi-component solid–liquid equilibrium model

At equilibrium, the solid phase fugacity for the *i*th component is equal to the liquid phase fugacity of the same component in solution.

$$f_1^i = f_s^i \tag{1}$$

The solid and liquid phase fugacities can be expressed as:

$$f_1^i = \phi_1^i x_1^i p \tag{2}$$

$$f_s^i = f_s^{0i} x_s^i \tag{3}$$

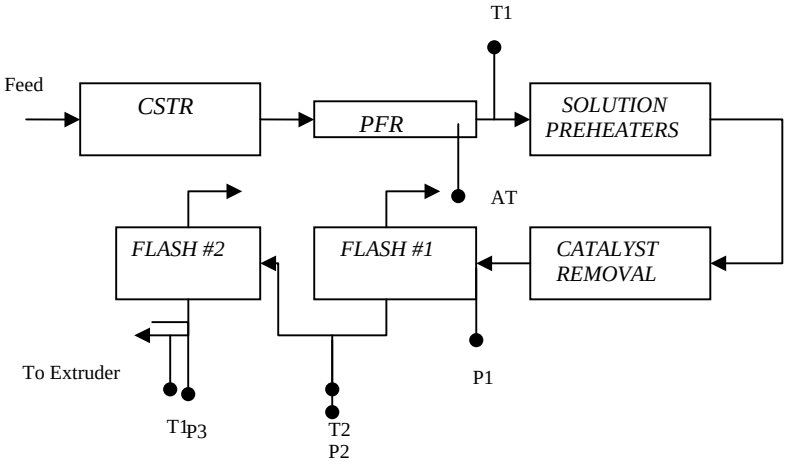

Fig. 1. Schematic flowsheet of a solution polymerization plant.

In the expression for solid phase fugacity it has been assumed that in the solid phase mixture there is no interaction effects between the components. Hence the partition coefficient k^i can be obtained as:

$$k^i = \frac{x_s^i}{x_l^i} = \frac{\phi_l^i p}{f_s^{0i}} \tag{4}$$

Dividing both the numerator and denominator of Eq. (4) by the fugacity of the pure subcooled liquid *i*th component, the following expression for the partition coefficient is obtained as:

$$k^i = \frac{(\phi_l^i p / f_l^{0i})}{(f_s^{0i} / f_l^{0i})} \tag{5}$$

The fugacity of the subcooled pure liquid *i*th component solute is expressed as:

$$f_l^{0i} = \phi_l^{0i} p \tag{6}$$

Using Eqs. (5) and (6) can be expressed as:

$$k^i = \frac{\phi_l^i p / \phi_l^{0i} p}{f_s^{0i} / f_l^{0i}} = \frac{\phi_l^i / \phi_l^{0i}}{f_s^{0i} / f_l^{0i}} \tag{7}$$

The fugacity of *i*th component in the solid state is obtained using a thermodynamic cycle (Pan and Radosz [1]):

$$\ln\left(\frac{f_l^{0i}}{f_s^{0i}}\right) = \frac{\Delta_{fus}H}{RT_{fus}}\left(\frac{T_{fus}}{T} - 1\right) + \frac{\Delta C_p}{R}\left(1 - \frac{T_{fus}}{T}\right) - \frac{\Delta C_p}{R}\ln\left(\frac{T}{T_{fus}}\right) + \frac{\Delta v}{RT}(p - p^{sat}) \tag{8}$$

All the terms in the Eq. (8) are not equally important [3]. The second and third terms tend to cancel each other while at low pressures the last term becomes insignificant. Hence at low pressures Eq. (8) can be simplified into:

$$\ln\left(\frac{f_l^{0i}}{f_s^{0i}}\right) = \frac{\Delta_{fus}H}{RT_{fus}}\left(\frac{T_{fus}}{T} - 1\right) \tag{9}$$

When *n*-alkanes with higher number of carbon atoms are heated they undergo a phase transition in the solid phase from stable crystalline structures to more unstable structures. For prediction of the solubility of these alkanes Eq. (9) has to be modified to the following form to account for phase transitions in the solid state [4,7,1].

$$\ln\left(\frac{f_l^{0i}}{f_s^{0i}}\right) = \frac{\Delta_{fus}H}{RT_{fus}}\left(\frac{T_{fus}}{T} - 1\right) + \frac{\Delta_{tr}H}{RT_{ss}}\left(\frac{T_{tr}}{T} - 1\right) + \frac{\Delta v}{RT}(p - p^{sat}) \tag{10}$$

where T_{tr} is the temperature where the transition takes place below the melting point of the solid. For polymer solvent systems Eq. (8) has been modified by Pan and Radosz [1] to the following expression as:

$$\ln\left(\frac{f_l^{0i}}{f_s^{0i}}\right) = \left(\frac{\Delta_{fus}H}{RT_{fus}}\left(\frac{T_{fus}}{T} - 1\right) + \frac{\Delta v \mathrm{PM}_{mon}}{RT_{fus}}\right) cn \tag{11}$$

where c is the fraction of crystallinity of the polymer, n the number of monomer units in the polymer backbone and M_{mon} the molecular weight of the monomer, Δv the difference between the specific volume of the amorphous and crystalline polymer and can be calculated as:

$$\Delta v = \frac{1}{\rho_a} - \frac{1}{\rho_c} \tag{12}$$

where ρ_a and ρ_c are the densities of the amorphous and crystalline forms of polymer. For polyethylene, ρ_a and ρ_c has been taken to be 853 and 1004 kg/m^3, respectively [1]. It should be mentioned here that the term c can be used as parameter in the model since they vary between polymer grades. $\Delta_{fus}H$ is the heat of fusion for one ethyl unit in Eq. (11) and has been taken to be equal to 8.22 kJ/mol [1]. Nakasone et al. [8] and Dirand et al. [19] have shown that the melting point of *n*-alkanes tends to become constant at high molecular weights and the convergence temperature is estimated to be 414.3 K. However, the model presented in

Table 1
Pure component parameters of PC–SAFT equation of state

Component	m	α (Å)	ε (K)
C_{12}	5.3060	3.8959	249.21
C_{13}	5.6877	3.914	249.7
C_{14}	5.9002	3.9396	254.21
C_{15}	6.2855	3.9531	254.14
C_{16}	6.6485	3.9552	254.7
C_{17}	6.9809	3.9675	255.65
C_{18}	7.3271	3.9668	256.2
C_{19}	7.7175	3.9721	256
C_{20}	7.9849	3.9869	257.75
C_{21}	8.288436	3.981236	259.1913
C_{22}	8.630424	3.98516	259.6546
C_{23}	8.972305	3.98876	260.0788
C_{24}	9.329961	3.992221	260.4858
C_{32}	12.046	4.0114	262.726
Cyclohexane	2.5303	3.8499	278.11
Ethylene	1.593	3.445	176.47
Propane	2.002	3.6184	208.11
M-Xylene	3.1861	3.7563	283.98
PE-50	2.1670	3.6529	214.3028
PE-100	3.4645	3.8269	239.9809
PE-300	8.3861	3.9824	259.3279
PE-500	13.2649	4.0173	263.4113
PE-1000	25.4429	4.0443	266.5206
PE-2000	49.7869	4.05805	268.0903
PE-3000	74.1283	4.0627	268.6157
PE-5000	122.8093	4.0664	269.0369
PE-7000	171.4898	4.0679	269.2176
PE-8000	195.83	4.0685	269.2741
PE-9000	220.17	4.0688	269.318
PE-10000	244.5101	4.0692	269.3532
PE-15000	366.2104	4.0701	269.4588
PE-20000	487.9105	4.0706	269.5115
PE-30000	731.3107	4.07106	269.5643
PE-50000	1218.1108	4.0714	269.6066
PE-70000	1704.9108	4.0716	269.6247
PE-100000	2435.1109	4.0717	269.6383
PE-300000	7303.1109	4.0719	269.6594
PE-500000	12171.111	4.07194	269.6636

Table 2
Melting point data of components

Component	T_{fus} (K)
PE-50 [17]	110
PE-100 [17]	182.6
PE-300 [17]	314.0
PE-500 [9]	347.66
PE-1000 [9]	378.18
PE-2000 [10]	400.0
PE-3000 [10]	408.0
PE-5000 [10]	413.0
PE-7000 [10] and higher MW polymer	414.0

the present study is for polydisperse polyethylene and hence pseudo-component approximation has been introduced for proper characterization of the polymer. Melting point data for low molecular weight pseudo-components were obtained from Takamizawa et al. [9]. A more detailed discussion regarding melting point variation of linear polyethylene with chain length is also available [10]. Melting point temperatures of linear polyethylene pseudo-components used in this work are given in Table 2.

Using PC–SAFT equation of state, the fugacity coefficients ϕ_l^i and ϕ_l^{0i} in Eq. (7) are calculated. For solving the multi-component SLE problem the following equation is solved as:

$$\sum (k^i x_l^i - 1) = 0 \tag{13}$$

A detailed discussion about PC–SAFT has been presented by Gross and Sadsowski [5,6]. Three pure component parameters are needed for PC–SAFT namely segment number, segment diameter and attraction parameter. The values of these parameters used in this work are given in Table 1. The pure component parameters for high molecular weight linear polyethylene pseudo-components have been extrapolated from those of *n*-alkane homologous series [5].

4. Results and discussions

4.1. Validation of model

The equation of state approach, using various equation of states, has already been validated on experimental data. However, the applicability of PC–SAFT EOS in the SLE framework has not been tested before. Hence the model has been tested on available experimental data and the results have been presented in this section. The model parameters (fractional crystallinity and binary interaction parameters) are adjusted by matching the experimental data. The enthalpy of fusion per ethyl unit (8.22 kJ/mol) is assumed to be constant for all the pseudo-components of polyethylene.

4.2. Solubility predictions for n-alkanes in n-hexane

The experimental data of Hoerr and Harwood [11] on the solubility of *n*-dodecane, *n*-hexadecane, *n*-dotriacontane in *n*-hexane have been used for matching the predictions of the model. Pure component data of the *n*-alkanes necessary for predictions like, melting point, solid–solid transition temperatures, etc. were collected from Pauly et al. [15] and the NIST chemistry webbook database [18]. Both sets of data were used for predictions and the results are presented in Fig. 2. The dashed curves are results based on the data of NIST, whereas the solid curves are based on the data of Pauly et al. [15]. The figure shows that the temperature at which the alkanes dissolve in hexane increases with the rise of molecular weight of the alkane. For *n*-alkanes, which showed solid–solid transition below the melting point temperature, Eq. (10) had to be used for calculation of solubility. The solubility data was correlated at atmospheric pressure and hence the pressure term in Eq. (10) was neglected. From Fig. 2, it is observed that for *n*-hexadecane, the predictions based on the data of Pauly et al. [15] under predict the SLE temperature. This is because Pauly et al. [15] have suggested solid–solid transition of all *n*-alkanes above C_{16} (including C_{16}), whereas NIST data suggests no solid–solid transition of even *n*-alkanes (like C_{14}, C_{16}, etc.) upto C_{20}. Thus, it is observed that by accounting for solid–solid transition of *n*-hexadecane, the predictions deteriorate. Phase behavior of *n*-alkane mixtures are suitably predicted by PC–SAFT by taking zero or very low values of binary interaction parameters [5]. Hence in this work, for *n*-alkane systems, binary interaction parameters have been set to zero. However, the real utility of this model cannot be judged from the prediction of alkane solubility because even simpler EOS or models have been found to be equally accurate [2].

4.3. Solubility predictions for polyethylene-solvent systems

The experimental data on the solubility of polyethylene in M-xylene as reported by Richards [12,13] has been used for prediction purpose. Eq. (11) was used in correlating the solubility and the pressure dependency term was omitted from the expression as the solubility data [12,13] are at atmospheric pressure. Fig. 3 shows that the experimental results matched reasonably well with the calculated values. As reported by Richards [12], the molecular weight of the polyethylene was taken to be equal to 17,000. However, as will be discussed later, a proper molecular weight distribution (MWD) of polymer is required for accurate predictions of SLE temperatures. The predictions were done, by taking the polymer to be monodisperse and hence the system was assumed to be binary. Binary interaction parameter was adjusted to −0.003 and fractional crystallinity was 0.7.

4.4. Prediction of wax precipitation temperatures from multi-component paraffin system

The predictions shown earlier were based on binary systems. To check the performance of the model on multi-component systems, a synthetic mixture of heavy *n*-paraffins

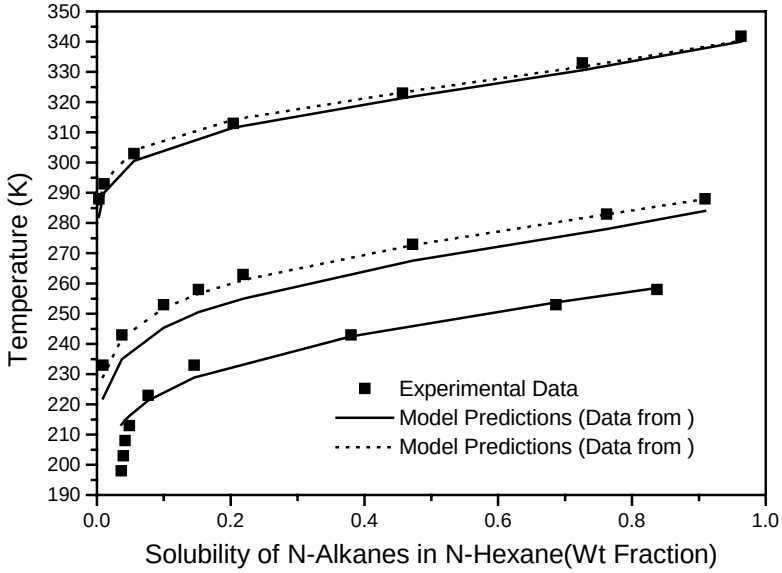

Fig. 2. Solubility of *n*-dodecane, *n*-hexadecane, and *n*-dotriacontane in *n*-hexane.

was selected. Crude oils and condensate gases contain long-chain *n*-alkanes, which can precipitate as waxes and present problems by clogging the pipelines. To prevent the phase split from happening, the crude oil or gas mixture temperature has to be maintained above the wax appearance temperature (WAT). Hence proper prediction of the wax appearance temperatures is a key to the solution of the problem. The composition of the synthetic mixtures (M1–M9) and experimental data were obtained from Daridon et al. [14]. In this case too, two sets of pure component data [15,18] were used and Table 3 presents the experimentally observed and calculated WAT, using both the sets of data. It is observed that with the increase in the number of components in the mixture, the

Table 3
Experimental and calculated wax appearance temperatures in a synthetic paraffins system

Mixture	Experimental [14]	Calculations [18]	Calculations [15]
M1	270.6	273.84	271.24
M2	273.7	276.26	274.98
M3	277.0	281.75	278.87
M4	279.1	284.51	282.75
M5	283.4	289.23	286.6
M6	286.1	291.87	289.95
M7	289.9	296.12	293.75
M8	295.9	301.87	299.97
M9	301.6	308.01	306.1

Calculations were based on pure component data from two sources [15,18].

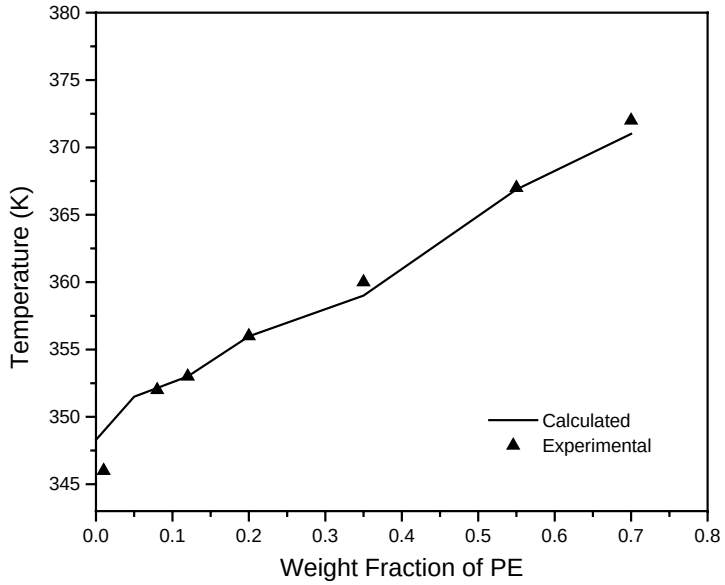

Fig. 3. Solubility of polyethylene (PE 17,000) in M-xylene.

deviations between the experimental and calculated values tend to increase. This model assumes that there is no interaction among the various components of the precipitated solid and this deviation may be attributed to that assumption.

4.5. Prediction of solution polymerization SLE

The objective of this section is to predict the effects of various solution polymerization process conditions on SLE of polyethylene and then to propose an algorithm for real-time prediction of SLE phase boundaries. Among the various process conditions, the presence of ethylene and polymer polydispersity are the most important factors which may cause significant deviations from the conventional model of considering polymer solutions as a binary mixture of polymer and solvent. Linear low density polyethylene (LLDPE) can be produced by either the gas, slurry or solution phase process, using Ziegler Natta catalysts and each process has got its own advantages and disadvantages [16]. As far as phase equilibria is concerned, SLE plays an important role in slurry phase and solution phase reactions. A conventional solution polymerization unit consists of a reactor train followed by a heater for preheating the solution before it is fed to the flash columns operating at different pressures. An adsorber for the removal of catalyst from solution is used before the flash columns. Throughout this entire operation polymer precipitation is highly undesirable, as this may result in choking and fouling of pipes thus reducing the efficiency of the process. The primary purpose of the flash columns is to recover unconverted ethylene and the solvent. As will be shown later this has a profound effect on the solid–liquid phase boundary of the system. In the subsequent predictions, the polymer has been assumed to be linear straight chain polyethylene with no short branches and which has a polydispersity index of about 2. Even though the property of the polymer produced by Ziegler Natta catalysts differs from the polyethylene assumed here, much insight can be gained about the SLE of solution polymerization process from this work. The solvent used in the simulation runs is cyclohexane and the polymerization reactor pressure is taken as 150 bar.

4.5.1. Effect of monomer

In a tubular reactor, as reaction proceeds, the ethylene concentration decreases continuously along the length of the reactor, while the polymer concentration rises steadily. Fig. 4 has been drawn assuming that ethylene is constantly being depleted from the system and polymer concentration is increasing. The system considered is ternary in nature consisting of ethylene, cyclohexane and polyethylene. Cyclohexane is used in the system as a solvent and hence it does not take part in the reaction. Initial weight fraction of ethylene is taken as 0.51, while that of polyethylene is taken to be very small (but not 0). Final weight fraction of ethylene at the exit of the reactor is 0.08, while that of polyethylene is 0.43. Weight fraction of cyclohexane in the system is constant at 0.49. Average molecular weight of the polyethylene is taken as 50,000. It is evident from Fig. 4 that polymer precipitation temperature increases drastically if the feed ethylene concentration is very high. The high dissimilarity between the ethylene and polymer molecules causes ethylene to reject the polymer from the solution. However, it must noted that the solution here has been assumed to be ternary and a low initial ethylene: solvent ratio may prevent the steep rise of precipitation temperature. In other words the curve will be of the type of curve ABC in Fig. 4 with the section AD missing. In that case, the precipitation curve will be almost qualitatively identical to that of the dashed curve in Fig. 4 which has been simulated in the absence of monomer in

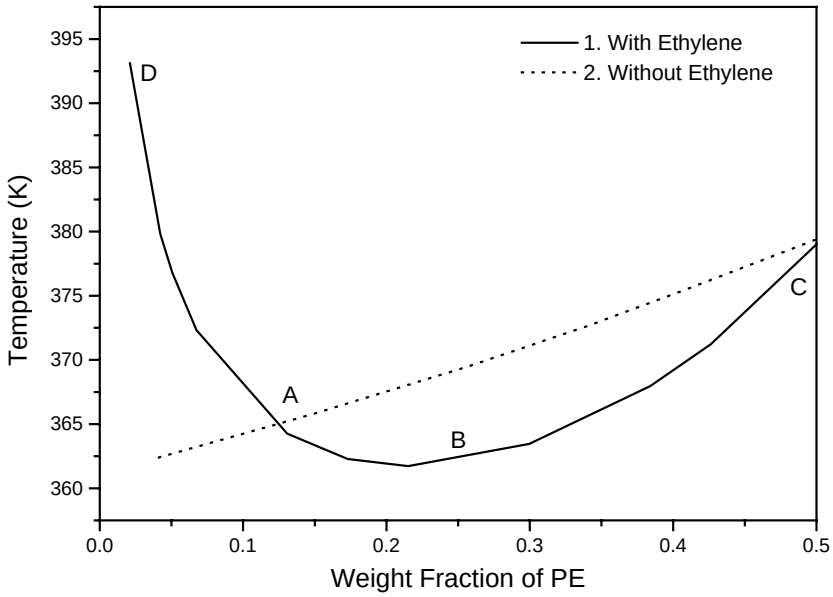

Fig. 4. Solubility curve of polyethylene (PE 50 k) in a ternary (cyclohexane, ethylene, and PE) system.

the solution. While simulating the dashed curve, the system is considered to be binary (polyethylene and cyclohexane), with the polymer concentration rising from a small value to 0.49 and the solvent decreasing continuously. From the dashed curve, it is evident that the presence of cyclohexane serves to keep down the precipitation temperature of polyethylene. It also serves as a heat sink, with much of the heat liberated due to polymerization being taken up by the large presence of the solvent. However, it is interesting to note that after point A in Fig. 4 the precipitation temperature of polymer in the solution in presence of ethylene goes below that of the temperature where polymer precipitates without ethylene. This implies that at lower concentrations ethylene acts as a co-solvent, while at higher concentrations it acts as an anti-solvent.

In the ternary system, it can be visualized that the steep temperature rise at very low polymer concentrations is due to the presence of a large concentration of ethylene in the solution. However, as ethylene decreases in the system, the precipitation temperature decreases and ultimately the solid and the dashed curves converge again. Generally reactors never operate in a region where the steep temperature rise (represented by curve AD) occurs and hence this places a limit to the maximum ethylene: solvent ratio that can be used in the reactors. Hence the maximum probability of polymer precipitation remains at the outlet of the reactors. If a plug flow reactor is used as the first reactor in the reactor train, then the feed solution must be preheated to prevent polymer phase split in the reaction media. However this may be overruled in the case of continuous stirred tank reactors, as the solution in the reactor is well mixed and the feed solution is almost instantaneously heated up the moment it enters the CSTR due to the highly exothermic polymerization reactions.

4.5.2. Effect of polymer polydispersity

For simulating the effect of polymer polydispersity in the reaction mixture the polyethylene is characterized into pseudo-components. The MWD of the polyethylene considered is presented in Table 4. The solubility curves for a polydisperse polyethylene and monodisperse polyethylene (with molecular weights equal to the number average and weight average molecular weights) in cyclohexane are shown in Fig. 5. It is observed that for higher molecular weights of monodisperse polymer, the solubility curve almost coincides with that of the curve for polydisperse polymer. Generally when the question of characterization of a polydisperse polymer into a single component arises, the number average molecular weight is chosen as the characterization factor. But in SLE of polymers this can lead to under-prediction of precipitation temperature. Hence from the modeling point of view, one can obtain accurate results if the polydisperse polymer is represented by a monodisperse polymer, with molecular weight equal to that of the molecular weight of the heaviest pseudo-component in the polydisperse polymer. Tables 4 and 5 show the pseudo-component characterization of the inlet polydisperse polymer and the precipitated solid respectively. Even though the weight fraction of the pseudo-component of molecular weight 300,000 is negligible in the polymer, it is observed from Table 5 that, the polymer precipitated is almost entirely comprised of it. The lower molecular weights still remain in the liquid phase. This implies that, the heaviest fraction of the polymer pseudo-component precipitates out first from the solution and it solely governs the point of phase separation.

Table 4
MWD of polyethylene characterized by pseudo-components

Pseudo-component	Weight fraction
PE-50	1.87384E-5
PE-100	9.29211E-5
PE-300	3.84777E-4
PE-500	0.00107
PE-1000	0.00462
PE-2000	0.01144
PE-3000	0.02275
PE-5000	0.04446
PE-7000	0.04969
PE-8000	0.05306
PE-9000	0.06314
PE-10000	0.07972
PE-15000	0.14338
PE-20000	0.1699
PE-30000	0.20818
PE-50000	0.11097
PE-70000	0.03101
PE-100000	0.00611
PE-300000	1.20399E-6
PE-500000	9.39991E-14

4.6. Real-time simulation of polymer SLE

Real-time models are always directly synchronized with the plant by hooking up the simulation package online with

Table 5
MWD of precipitated polyethylene characterized by pseudo-components

Pseudo-component	Weight fraction
PE-50	9.12696E-12
PE-100	8.68836E-11
PE-300	2.28564E-9
PE-500	6.48182E-9
PE-1000	2.98554E-8
PE-2000	3.44525E-7
PE-3000	3.4291E-6
PE-5000	5.17525E-5
PE-7000	1.36846E-4
PE-8000	1.55281E-4
PE-9000	1.98774E-4
PE-10000	2.66515E-4
PE-15000	6.71263E-4
PE-20000	0.00111
PE-30000	0.00264
PE-50000	0.00541
PE-70000	0.00564
PE-100000	0.00833
PE-300000	0.93105
PE-500000	0.04435

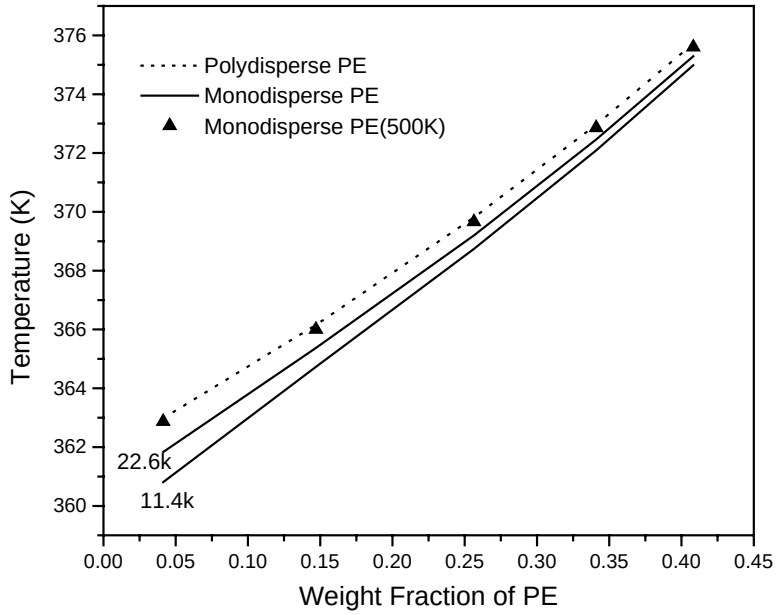

Fig. 5. Solubility curves of monodisperse and polydisperse polyethylene in cyclohexane.

the plant distributed control system. The model is expected to pick up data from the plant DCS and uses it as the input to the simulation package. There is a specific timeframe within which the entire model must be solved for the real-time prediction of process conditions. Here the model acts as a virtual software sensor and most of its advantage over actual hardware sensors lies in its flexibility and ease of use. For the solution of the model by standard modern day computers in the given time limit, rigorous models may not be always used. Also the solid–liquid phase equilibria may not be the only simulation that is going on real-time. The SLE calculations may be accompanied by other inferential property prediction calculations, which further increase the CPU overhead. Hence application of a simplified model without losing sufficient accuracy of predictions becomes important.

It has been shown earlier how ethylene plays a major role in the reactors and by ignoring it in SLE predictions of reactors, much of the accuracy will be lost. But Fig. 4 also shows how with decreasing ethylene concentration (increasing polymer concentration), the effect of ethylene in the solution is gradually lost. Also Fig. 5 shows that by characterizing the polydisperse polymer as a monodisperse polymer with molecular weight equal to the highest pseudo-component fraction, predictions remain almost equally accurate. Hence for predictions of reactor SLE a ternary system with the monomer, solvent and high molecular weight polymer would suffice.

If a very high initial ethylene concentration is not used, then among all equipment the solution preheaters preceding the flash columns remain the most susceptible to fouling due to solid deposition. After the first flash column almost all the monomer and about 50% of cyclohexane is lost as vapor from the solution. Fig. 6 shows the pressure–temperature curves, for the polymer solution before and after the first flash column. The system is considered to be ternary in the pre-flash zone (ethylene, cyclohexane, and polymer), while in the post-flash analysis, the system is considered to be binary (as almost all the ethylene has been flashed off, the system now only has cyclohexane and polyethylene). Along with the solid–liquid boundary, vapor–liquid phase separation curve has also been generated in the figure. The solid curve shows the phase split boundaries before the flash and the dashed curves show the same after the flash column. It is observed that the SLE curves have shifted to the right and the vapor–liquid equilibria (VLE) curves have shifted down after the solution has been flashed. This implies that the zone over which the solution remains in a single phase has reduced thus increasing the probability of a phase split.

Pressure–temperature isopleths like that of Fig. 6 can be generated in real-time and the exact position where the plant is operating can be mapped on the plot. This would enable plant operators to take preventive actions in case of emergencies when the real-time simulation warns them of a prospective phase split. It must be mentioned that, Fig. 6 has been predicted by assuming the molecular weight of the polymer to be 500,000 (as discussed earlier the highest MW of polymer pseudo-component is good enough). However, the fraction of polymer of molecular weight 500,000 and above, may be much less in the polydisperse polymer. Hence when the SLE phase boundary is breached, one may not find a drastic deposition of polymer in the pipe lines. However, as more of the solution enters the solid–liquid zone, more polymer of lower molecular weights will start precipitating out. Fig. 6 also shows that the SLE curve is almost vertical (with a slight positive slope) showing that it has got little variation with pressure. Hence temperature is the parameter

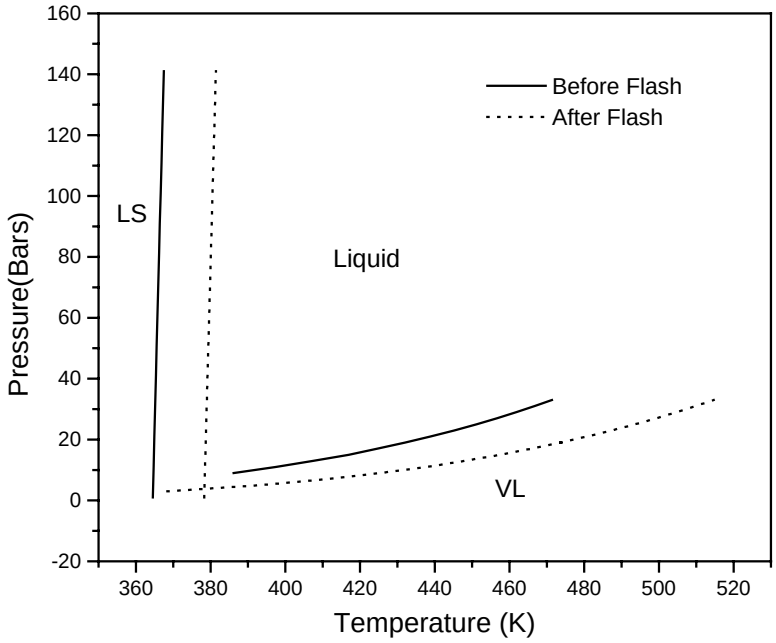

Fig. 6. Pressure–temperature curves of polyethylene before and after the flash column.

which should be controlled for prevention of polymer precipitation.

The significance of the real-time model is further emphasized if the results of the simulation experiment are studied. In the experiment a disturbance is simulated in the plant where a sudden drop in conversion occurs. This may happen in a plant due to a variety of reasons including catalyst poisoning or catalyst pump malfunctioning etc. Due to the drop in conversion a very sharp drop in reaction temperature occurs in the CSTR. With loss in conversion the polymer concentration also decreases in the solution. From Fig. 4 we observe that under these conditions the system shifts from the region BC–AD. Hence there is a sharp rise in the SLE phase split temperature. Fig. 7 shows such a scenario where the SLE phase split temperature exceeds the reaction temperature and solid polymer separates out of the solution. The temperature of the reactor shown is the outlet of the PFR (temperature indicator T1 of Fig. 1). In the experiment done it is assumed that during the plant disturbance the property of the polymer produced in the reactor is unchanged. It must

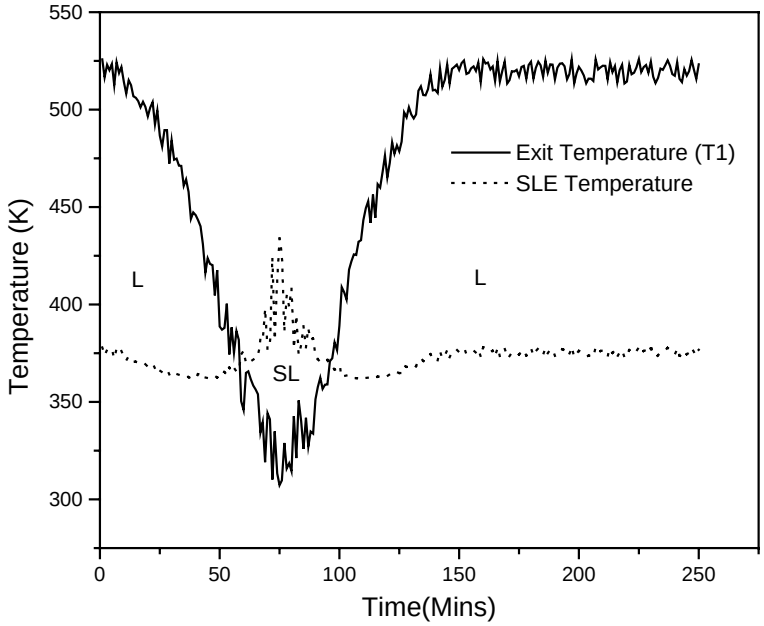

Fig. 7. Simulation experiment results.

be remembered that the feed to the CSTR is not preheated and hence under reaction loss, the chance of a phase split is more in such cases. The real-time model provides valuable insights in such situations and helps the plant operators in taking corrective actions.

5. Conclusion

An algorithm for the real-time prediction of SLE in solution polymerization of polyethylene was developed. Available literature characterizes the polymer as a monodisperse polymer with an average molecular weight. In this work, multi-component SLE was studied where the polymer polydispersity was taken into account. The studies revealed that, instead of lumping the polymer with an average molecular weight, the polymer should be characterized with the highest molecular weight fraction of the polydisperse polymer. The effect of monomer on the SLE characteristics of the polymer solution was also studied. The results obtained from the study were applied in developing the real-time model. A simulation experiment was also done where the importance of such real-time models was highlighted.

Acknowledgements

Financial help received from the MHRD project number F.27-1/2002-TS.V dated 19/03/2002 is thankfully acknowledged.

Appendix A. Nomenclature

Å	angstroms
c	fraction of polymer crystallinity
ΔC_p	difference of heat capacity of solute in the solid and liquid state, $C_p^l - C_p^s$ (J/mol)
CSTR	continuous stirred tank reactor
f	fugacity
EOS	equation of state
$\Delta_{fus}H$	enthalpy of fusion (J/mol)
$\Delta_{tr}H$	enthalpy of solid-solid transition in n-alkanes below melting point (J/mol)
k	partition coefficient
LLDPE	linear low density polyethylene
MWD	molecular weight distribution
M_{mon}	molecular weight of monomer
n	number of ethyl units in a linear polyethylene chain
p	pressure
p^{sat}	saturation pressure
PE	polyethylene
PC–SAFT	perturbed chain statistical associating fluid theory
R	universal Gas constant,
SLE	solid–liquid equilibria
T	temperature (Kelvins)
T_{fus}	normal melting point
T_{tr}	temperature of solid–solid transition below melting point for n-alkanes
x	mole fraction
Δv	difference of volume of solute in the solid and liquid state, $v_l - v_s$ (m^3/mol)
VLE	vapor–liquid equilibria
WAT	wax appearance temperature

Greek letters

ϕ	fugacity coefficient
ρ	density

Subscripts

l	liquid phase
s	solid phase
a	amorphous
c	crystalline
m	melting
ss	solid–solid phase transition
mon	monomer

Superscripts

i	component in a mixture
$0i$	pure component

References

[1] C. Pan, M. Radosz, Fluid Phase Equilib. 155 (1999) 57–73.
[2] C. Peng, H. Liu, Y. Hu, Fluid Phase Equilib. 180 (2001) 299–311.
[3] J.M. Prausnitz, R.N. Lichtenthaler, E.G. Azevedo, Molecular thermodynamics of fluid phase equilibria, second ed., Prentice-Hall, Englewood Cliffs, NJ, 1986.
[4] J.A.P. Coutinho, Fluid Phase Equilib. 158–160 (1999) 447–457.
[5] J. Gross, G. Sadsowski, Ind. Eng. Chem. Res. 40 (2001) 1244–1260.
[6] J. Gross, G. Sadsowski, Ind. Eng. Chem. Res. 41 (2002) 1084–1093.
[7] J.A.P. Coutinho, S.I. Anderson, E.H. Stenby, Fluid Phase Equilib. 117 (1996) 138–145.
[8] K. Nakasone, Y. Urabe, K. Takamizawa, Thermochim. Acta 286 (1996) 161–171.
[9] K. Takamizawa, Y. Ogawa, T. Oyama, Polym. J. 14 (1982) 441–456.
[10] G. Allen, J.C. Bevington, Comprehensive Polymer Science, first ed., Pergamon, Headington Hill Hall, Oxford 0X30BW, UK.
[11] C.W. Hoerr, H.J. Harwood, J. Org. Chem. 16 (1951) 779–791.
[12] R.B. Richards, Trans. Faraday Soc. 42 (1946) 10–20.
[13] R.B. Richards, Trans. Faraday Soc. 42 (1946) 20–28.
[14] J.L. Daridon, J. Pauly, M. Millet, Phys. Chem. Chem. Phys. 4 (2002) 4458–4461.
[15] J. Pauly, J.L. Daridon, J.A.P. Coutinho, N. Lindeloff, S.I. Anderson, Fluid Phase Equilib. 167 (2000) 145–159.
[16] C. Kiparissides, Chem. Eng. Sci. 51 (1996) 1637–1659.
[17] R.C. Reid, J.M. Prausnitz, B.E. Poling, The Properties of Liquids and Gases, fourth ed., McGraw-Hill, New York, 1988.
[18] NIST Chemistry Webbook, http://www.nist.gov/srd.
[19] M. Dirand, M. Bouroukba, A.J. Briard, V. Chevallier, D. Petitjean, J.P. Corriou, J. Chem. Thermodyn. 34 (2002) 1255–1277.
[20] S. Behme, G. Sadowski, Y. Song, C. Chen, AIChE J. 49 (1) (2003) 258–268.
[21] F. Tumakaka, J. Gross, G. Sadowski, Fluid Phase Equilib. 194–197 (2002) 541–551.